1   **Monitoring and evaluation of sand nourishments on an**

2   **embayed beach exposed to frequent storms in eastern China**

3   Junli Guo[a], Lianqiang Shi[b], Shunqi Pan[c], Qinghua Ye[d], Wufeng Cheng[a], Yang Chang[a],

4   Shenliang Chen[a,*]

5   [a] *State Key Laboratory of Estuarine and Coastal Research, East China Normal*

6   *University, Shanghai 200241, China*

7   [b] *Second Institute of Oceanography, Ministry of Natural Resources of China, Hangzhou*

8   *310012, China*

9   [c] *Hydro-environmental Research Centre, School of Engineering, Cardiff University,*

10   *Cardiff CF24 3AA, UK*

11   [d] *Deltares, Delft 2614HV, the Netherlands*

12   [*]Corresponding author.

13   *E-mail address*: slchen@sklec.ecnu.edu.cn (S. Chen)

14

15

16

17

18

19

20

Abstract

Beach nourishment is a proved effective protection approach which has been widely used in recent years. An Argus video monitoring system has been set up to monitor morphological changes and effects of continuous nourishments at Dongsha beach, an embayed beach in Zhoushan Archipelago, eastern China. Video-derived shorelines along with their morphological parameters, such as dry beach width, dry beach area, beach orientation and unit width volume were analyzed during the monitoring period from June 2016 to July 2017. Analysis of video monitoring data shows that shorelines retreated during autumn and winter when storms were intensive, while advanced in spring and summer, with a lot of bulges occurred after nourishment projects. Abrupt variations in the beach orientation were always followed by gradual recoveries to the average beach orientation, while continuous counter-clockwise rotation occurred after March, 2017 when storm events were sparse. Comparing the different beach responses to individual storm events, we found that small-scale and short-interval sand nourishment implemented timely after storms can compensate for sediment loss more effectively on this beach. This study can provide a reference for local beach management.

Keywords: Argus video monitoring; beach nourishment; storm erosion; occurrence time of nourishment; beach management

1. Introduction

Due to the global climate change with sea level rise and more frequent and severe storms, serious beach erosion is observed all over the world (Castelle et al., 2007; Houston and Dean, 2014; Qi et al., 2010; Scott et al., 2016; Smith et al., 2014). At least 70% of sandy beaches experienced widespread erosion around the world (Bird, 1985), and approximately 50% of sandy coasts were regressed in erosion in China (Third Institute of Oceanography, 2010). Under this circumstance, there are growing numbers of beach protection or restoration projects in China, particularly in the tourism hotspots, to meet increasing public requirements (Kuang et al., 2011).

The common approach adopted in the past to protect or restore beaches is the hard engineering based (Cai et al., 2011; Pan, 2011). Although hard engineering, such as artificial coastal structures, can effectively mitigate shoreline retreat caused by storms, it may have negative impacts on its adjacent beach (Hamm et al., 2002). For decades, beach nourishment has become a preferred method to protect beaches in developed countries (Castelle et al., 2009; Cooke et al., 2012; Hamm et al., 2002; Hanson et al., 2002; Pan, 2011), which has also been frequently applied in China in recent years (Luo et al., 2016).

However, beach nourishments can often cause large-scale nearshore disturbances that affect the balance of alongshore and cross-shore sediment transport (Dean, 1983). Under natural conditions, storm-eroded sandy beaches may recover gradually over seasons to a decade timescale (Harley et al., 2015; Scott et al., 2016), while the beach

3

63   processes with nourishment disturbance vary significantly (Elko et al., 2005; Seymour

64   et al., 2005). Previous studies focused on nourishments with regular frequency and

65   fixed implement timing in European countries (Hanson et al., 2002), the USA (Leonard

66   et al., 1989) and Australia (Cooke et al., 2012). However, the beach protection approach

67   at Zhoushan Archipelago in China is different due to frequent occurrence of storms. To

68   prevent the severe storm erosion and maintain the recreational beach, small-scale and

69   irregular nourishments have been frequently implemented and the occurrence time of

70   those nourishments is often close to the storm period. Up to the present, beach

71   morphodynamic evolution involved with this beach protection approach remains

72   unclear.

73   Understanding the self-adjustment of beaches after nourishments is important for

74   management (Elko and Wang, 2007), while there is always no regular monitoring of

75   changes in beaches after nourishments (Chiva et al., 2018; Leonard et al., 1989; Stauble,

76   1988). Video monitoring systems are proved to be adequate in detecting and quantifying

77   spatial and temporal beach responses (Archetti and Romagnoli, 2011). Especially,

78   Argus system has been widely used in beach morphodynamic research in recent

79   decades (Angnuureng et al., 2017; Balouin et al., 2013; Karunarathna et al., 2014).

80   Nourishment can be further evaluated based on the continuous imagery data

81   obtained by video monitoring. Beach morphological variations and longevity of

82   borrowed sediments are criteria to evaluate the effectiveness of beach nourishment (Liu

83   et al., 2019; Psuty and Moreira, 1992). Factors affecting the beach nourishment

84 longevity include parameters of nourishment projects and physical characteristics of

85 beaches. The former mainly includes sediment characteristics, such as grain size

86 distribution (Chiva et al., 2018; Pranzini et al., 2018; Stauble, 2007), mineral

87 component (Pagán et al., 2018), volume scale (Basterretxea et al., 2007; Stauble, 2007)

88 and spatial location (Karambas and Samaras, 2014) of borrowed sediments. The latter

89 consists of wave/wind regimes (Karambas and Samaras, 2014) and the native

90 morphological characteristics of beaches (Liu et al., 2019). Different combinations of

91 those factors will result in different nourishment impacts on the beach.

92 In this study, we selected Dongsha beach, a 1.5 km-long embayed sandy beach in

93 Zhoushan Archipelago of China, to observe its morphodynamics and evaluate the

94 effectiveness of nourishments. An Argus video monitoring system was used to record

95 variability of beach morphology. Beach morphological parameters including: dry beach

96 width, shoreline displacement, dry beach area, beach orientation and rotation, and unit

97 width volumetric change for more than a year were analyzed using Argus imagery data.

98 Beach responses to individual storm events in five different cases were also revealed in

99 detail. Based on morphological analysis, the evaluation of nourishment effectiveness

100 and factors affecting nourishment longevity were discussed. Beach nourishment

101 implications were proposed for further beach management.

2. Materials and methods

2.1. Study area

104 Approximately 50% of sandy coasts were regressed in erosion in China over past

several decades (Third Institute of Oceanography, 2010). Thus, a large amount of beach

nourishment projects have been accomplished along China's coast since the 1990s (Cai

et al., 2011; Kuang et al., 2019; Luo et al., 2016). Zhoushan Archipelago is a popular

tourism destination with more than 30 embayed beaches (Xia, 2014), at a location

connecting the Hangzhou Bay and the East China Sea. Typhoon is a common coastal

hazard affecting the Archipelago with a frequency of 6 times a year on average (Lu,

2010), which has a significant impact on beach morphology and even threatens the

tourism. Dongsha beach was selected as the study area, which is located at Zhujiajian

Island in Zhoushan Archipelago (Fig. 1a). It is an embayed beach bounded by headlands

with a total length of about 1500 m and is a typical tourism beach. To monitor the

detailed evolution of the beach, an Argus video monitoring system with six cameras

(Fig. 1a and Fig. 2) was installed on 2015.

Slope of Dongsha beach varies alongshore, with measured values between 2.9%

and 3.5%. The steepest transects were found at the northern beach and the southern

transects were the flattest (calculated according to Guo et al., 2018). The median grain

size (D_{50}) of sediments on the beach range between 0.15 mm and 0.38 mm (fine sand).

The beach sediments mainly come from the erosion of coastal rocks eroded by the wind

and wave (Cheng et al., 2014). There is no direct river input around the Dongsha beach

(Xia, 2014). Fine-grained sediments are rich in the adjacent sea area of the Zhoushan

Archipelago due to the coastal current induced southward transportation of sediments

from the Yangtze River(Hu et al., 2009; Li et al., 2018), and there is a sand-mud

126 transition located on the 5 m of isobath in the ajacent sea area of Dongsha beach (Cheng

127 et al., 2014). There were sand dunes in the backshore of the beach, while the

128 construction of the seawall has broken the balance of cross-shore sediment transport on

129 the beach (Cheng et al., 2014; Guo et al., 2018), further resulting in the disapperance

130 of dunes.

131 Tidal data provided by Shenjiamen tidal gauge station (29.93°N,122.3°E) shows

132 that tides are mainly semi-diurnal and the mean tidal range is 2.6 m. Wave

133 measurements were simultaneously obtained hourly by a wave buoy (29.8°N,122.5°E)

134 located about 12 km offshore in 20 m depth. The offshore wave climate is characterized

135 by low to moderate wave energy (mean H_{sig}≈0.82 m, T_{peak}≈6.2 s). Fig. 1b indicates the

136 overall wave rose for the buoy. The prevailing waves come from the East, and direction

137 of high waves range from Northeast to Southeast with a maximum significant wave

138 height of 3.1 m.

139
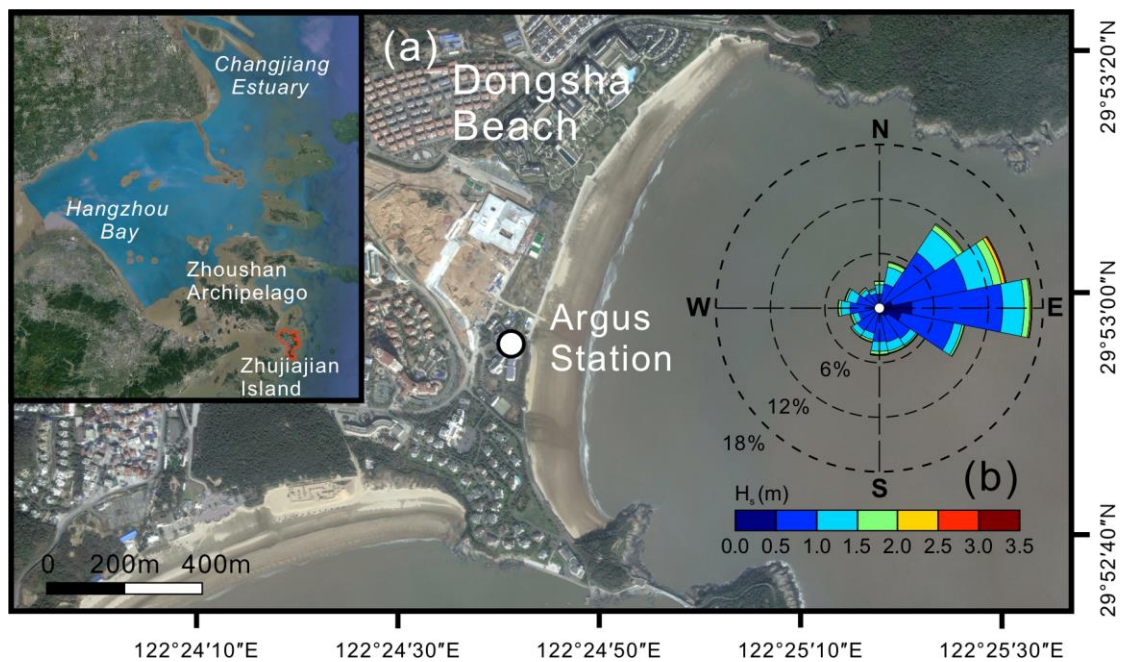
Fig. 1. Sketch of study area (a) and wave rose of the study area (b), in which H_s is the significant wave height. The satellite images obtained from Google Earth.

2.2. Beach nourishment

Seawall construction and the intensive storm events resulted in long-term erosion of Dongsha beach (Guo et al., 2018). To prevent storm erosion and widen recreational beach, beach nourishment projects were initiated in September 2016. Nourishment with irregular time, small scale and limited spatial distribution is the main beach maintenance pattern implemented on Dongsha beach, which is also common in China. The beach management department carried out 10 beach nourishment projects during 2016 and 2017 (Table 1, Fig. 2) with a total sand volume of ~52,000 m^3. The borrowed sediments were mainly placed in the area between transect 16 and transect 28, and the alongshore sand placement was limited in the area between transect 10 and transect 29 (Fig. 2) due to the restraints of transportation condition on the beach. All the nourishments have the same operations and materials which has the similar characteristics with the native sediments.

Table 1

Information of beach nourishments on Dongsha beach.

Nourishment	Time span	Sand volume (m^3)	Beach position
N1	9 Sep, 2016 - 13 Sep, 2016	~10000	Southern
N2	24 Sep, 2016	~1000	Southern
N3	29 Sep, 2016 - 30 Sep, 2016	~2000	Southern
N4	4 Oct, 2016 - 8 Oct, 2016	~5000	Southern
N5	31 Oct, 2016 - 10 Nov, 2016	~10000	Southern & Central
N6	5 Jan, 2017 - 13 Jan, 2017	~10000	Southern

N7	18 Jan, 2017 - 19 Jan,2017	~2000	Southern
N8	31 Jan, 2017 - 8 Feb, 2017	~10000	Southern
N9	18 Feb, 2017	~1000	Southern
N10	18 May, 2017	~1000	Southern

157

158
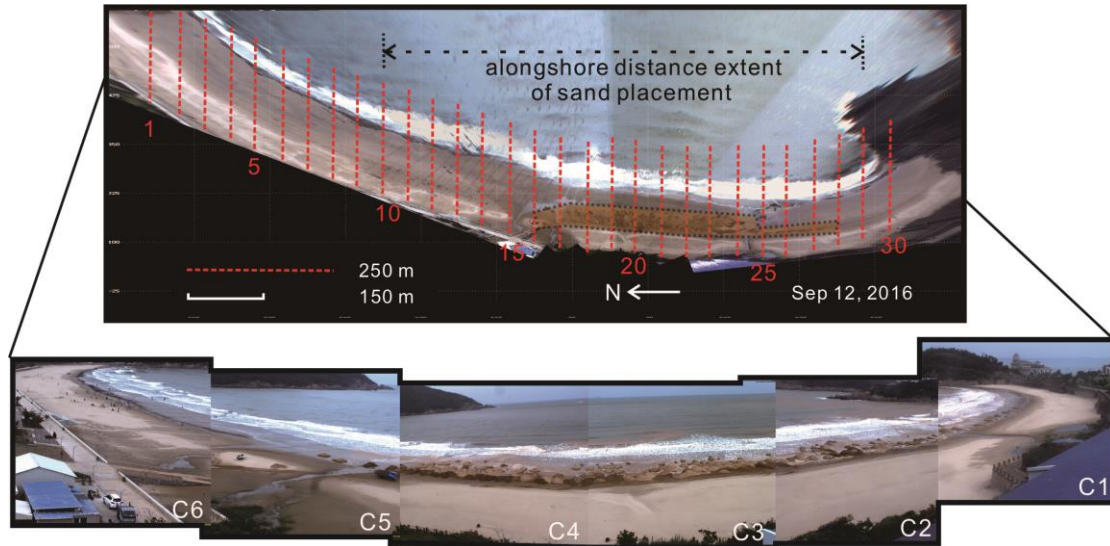
Fig. 2. Planview of Dongsha beach merged by snap images of six cameras (C1-C6) during N1 period (yellow shadow area shows the sand placement). 30 transects (red dotted lines) were set every 50 m on the beach surface from north to south (from y = 900 to y = -550), northward coordinates alongshore and eastward coordinates cross-shore with respect to Argus station are positive.

2.3. Identification of storm events

According to the method proposed by Boccotti (2000), storm events were identified when the significant wave height is greater than 1.5 times the annual average (0.82 m in this research) with duration ≥12 hours, which was based on the *in situ* data obtained by buoy. 19 storm events (S1-S19) were extracted during the study period from June 1, 2016 to July 1, 2017 (Fig. 3). Then, the wave energy storm peak E (m^{2}s)

170   was calculated as:

$$E = H_{max}^2 \cdot T_p \tag{1}$$

172   where H_{max} represents the maximum storm significant wave height, and T_p is the wave

173   period at the storm peak (Archetti et al., 2016; Harley et al., 2014; Senechal et al., 2015).

174   The storm power index P_s (m²h) (Dolan and Davis, 1992) was also calculated:

$$P_s = H_{max}^2 \cdot D \tag{2}$$

176   where D is the duration of "storm conditions" in hours.

177   *2.4.   Beach morphological variation processing*

178   Real-time and continuous imagery was extracted from the Argus video monitoring

179   system, with a frequency of 2 Hz in 10-min bursts every daylight half hour, including

180   Snapshot images, Timex images, and Variance images with a resolution of 2448×2048

181   pixels. To validate the accuracy of the beach morphology obtained by the Argus system,

182   a field survey was carried out at Dongsha beach on May 4, 2016 using RTK GPS, and

183   a total of 41 ground control points were measured. The results showed that the average

184   vertical error is 0.145 m, and more details were introduced by Guo et al.(2019).

185   The images from June 2016 to July 2017 were selected from the image dataset for

186   beach nourishment evolution analysis. All images of the months when the storm events

187   and sand nourishments were concentrated (September 1, 2016 - February 28, 2017)

188   were selected, and only partial images of the rest months were selected. Based on the

189   merged images of Argus cameras, 30 transects were set every 50 m on the beach from

190   north to south (from y = 900 to y = -550, Fig. 2). Then unit width volume change and

10

shoreline position of each transect were calculated in Argus Intertidal Bathymetry

Mapper module (Aarninkhof et al., 2003).

Dry beach width (*DBW*) can be calculated by shoreline position (Harley et al., 2014) as follows:

$$DBW_i = X_{shoreline,i} - X_{seawall,i} \tag{3}$$

where $X_{shoreline,i}$ is the position of shoreline obtained from Argus at transect *i*, and

$X_{seawall,i}$ represents the position of the seawall at transect *i*.

The alongshore-averaged dry beach width ($\overline{DBW}$, Harley et al., 2014) for the

beach was also calculated:

$$\overline{DBW} = \frac{1}{N} \sum_{i=1}^{N} DBW_i \tag{5}$$

where the number of transects *N* is 30.

Dry beach area (*DBA*) is an important parameter for the beach management, which

determines the space available for beach tourists. *DBA* can be approximately calculated

according to Harley et al. (2014) as:

$$DBA \approx \Delta S \sum_{i=1}^{N} DBW_i \tag{6}$$

where *ΔS* represents alongshore spacing between transects (*ΔS*=50 m).

Changes in shoreline position are often in response to sediment supply, sea level

rise, climate change, and human intervention (Karunarathna et al., 2018). In order to

describe the response of Dongsha beach over the study period, the mean distance *Δx*

(distance between shoreline of Jun 1, 2016 and later days in cross-shore direction during

the study period) was calculated according to Archetti et al. (2016) as:

212
$$\Delta x = \frac{\Sigma_i d_i}{n} \tag{7}$$

213 where i is the transect (i=1-30), d_i is the distance between shorelines in cross-shore

214 direction at each transect and n is the transect number (n=30. The previous field

215 investigation in Dongsha beach showed that 30 transects could represent the whole

216 beach in this study).

217 Shoreline variability is additionally influenced by beach rotation on embayed

218 beaches (Short and Masselink, 1999), and beach rotation is a key process for

219 understanding the morphodynamic of embayed beaches (Ojeda and Guillén, 2008).

220 Beach orientation and rotation were calculated according to Ojeda and Guillén (2008)

221 in this study, positive (negative) rotation value corresponds to a more clockwise

222 (counter-clockwise) orientation. A degree change in beach orientation means a 26 m

223 shoreline change of the two extremities in Dongsha beach.

224 Based on the morphological variation of the beach, the longevity of each

225 nourishment could be calculated. The longevity in this study represents the lasting

226 duration of borrowed sediments, it is the time duration when the mean unit width

227 volume is larger than that before the nourishment.

228 ## 3. Results

229 ### 3.1. Storm characteristics

230 A total of 19 storm events (S1-S19) were extracted during the study period from

231 June 1, 2016 to July 1, 2017 (Fig. 3). H_{max} and T_p, D, storm direction θ_p (wave direction

232 at the storm peak with respect to north), E and P_s were summarized for all the storm

233   events. The strongest storm event (S3) occurred in September 2016 with a P_s of 1157.76

234   m^{2}h, which is identified as significant severity ($P_s > 500$ m^{2}h) according to Mendoza et

235   al. (2011). Overall, four storm events over the study period were categorized as

236   significant, and three as moderate ($251 < P_s \leq 500$ m^{2}h), with the remaining 12 events

237   recognized as calm ($P_s \leq 250$ m^{2}h) (Fig. 3c). As shown in Fig. 3, storm events were

238   predominantly intensive in autumn (September - November), with a minority of calm

239   events occurring within the winter months (December - February). It can be seen that

240   peak direction of these storm events mainly distribute between north and east, with a

241   small number of storm events having a south direction.
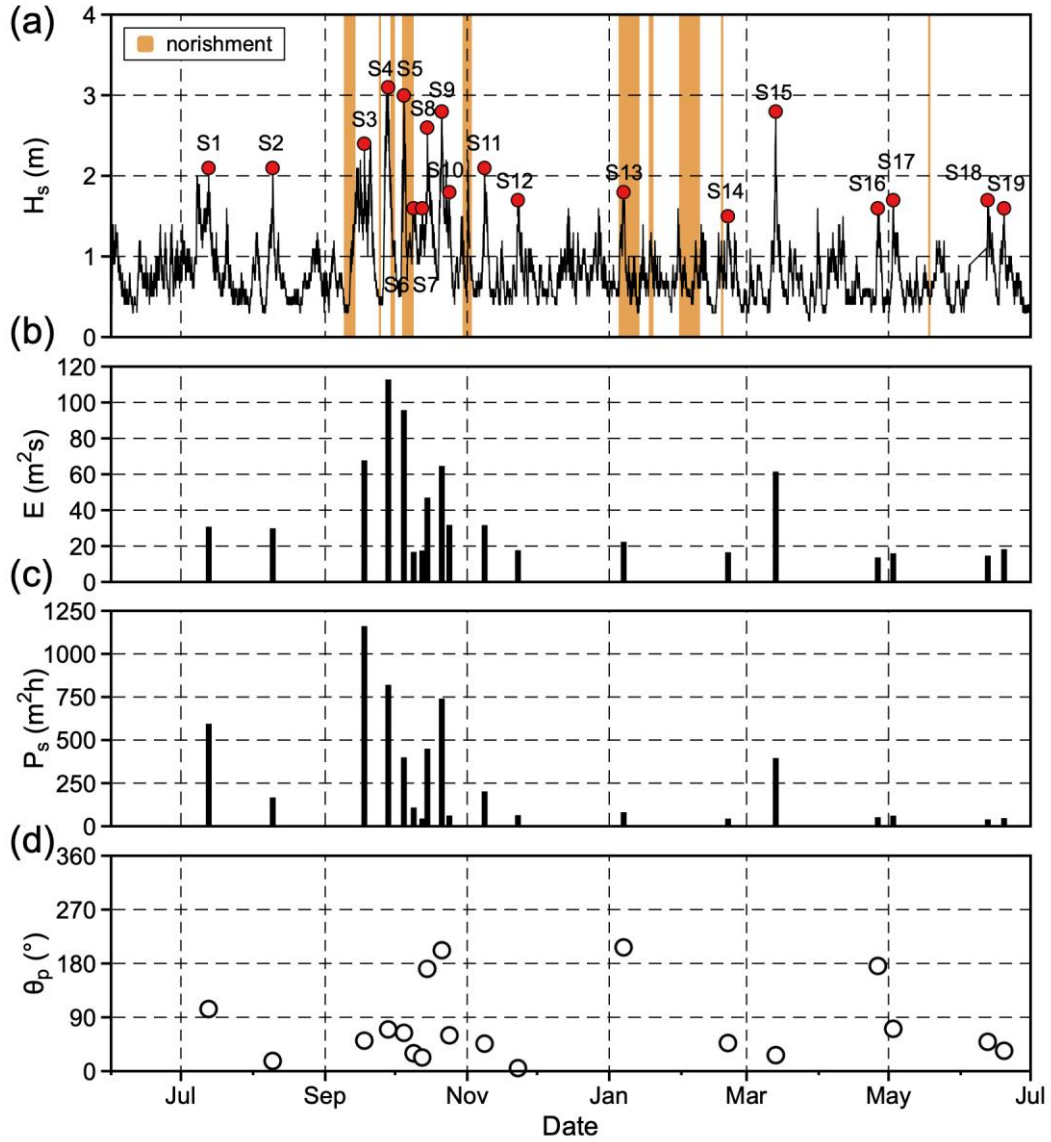
Fig. 3. Significant wave height (H_s) over the study period (**a**), storm energy E (**b**), storm power index P_s (**c**) and the peak direction θ_p (**d**) of each storm event. Red circles represent the peak significant wave heights during storm events, while the dark yellow shadow areas show the time span of each nourishment project.

3.2. Morphological variation of Dongsha beach

Averaged *DBW* at each transect was quantified for the beach over the study period as shown in Fig. 4. Since some transects (1-10 and 27-30) are not perpendicular to the

14

250   shoreline (Fig.2), calibrations of *DBW* at those transects were done (Fig. 4). Generally,

251   the northern part of the beach had the narrowest *DBW* while the middle part of the beach

252   had the widest *DBW* over the study period. *DBW* of Dongsha beach ranges from 76 m

253   (transect 8) to 138 m (transect 17). It is worth noting that the beach tourism facilities

254   are located on the area with larger *DBW* than the average (area between transect 13 and

255   transect 23), which is also the tourist-dense area.
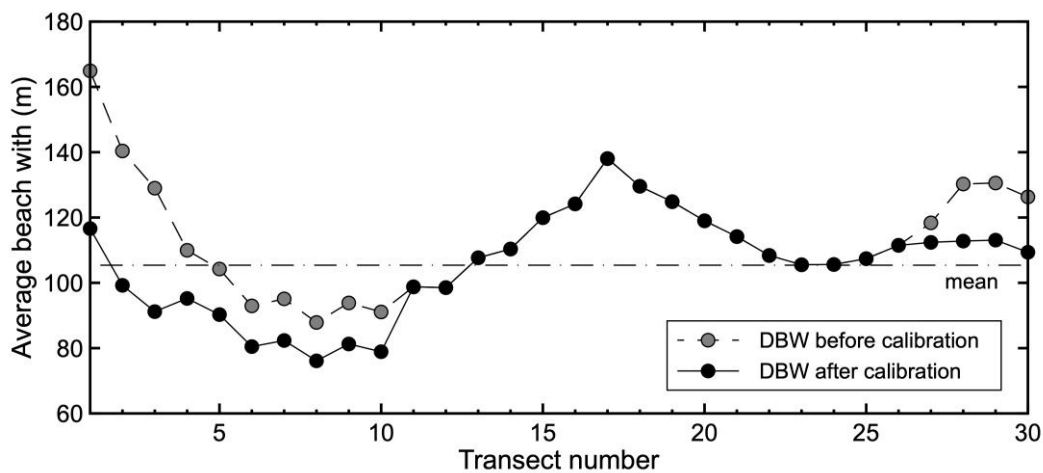
256

257   **Fig. 4.** Averaged dry beach width at each transect over the study period.

258   The majority of *Δx* values range generally between -25 and 20 m over the 13

259   months (Fig. 5a). There were a few higher positive values (from 20 to 49 m) came after

260   nourishments, and a few lower values occurred commonly in the storm-intensive period.

261   The largest shoreline retreat (-42.6 m) came after the last storm event during the storm-

262   intensive period, while the largest advance (49 m) occurred in the latter part of study

263   period without storm event. Temporal distribution of *Δx* values over the whole study

264   period suggests that shorelines retreated during autumn and winter while advanced in

265   spring and summer. It is worth noting that a lot of peak values occurred after

15

266 nourishment projects.

267   Temporal evolution of *DBA* has the similar pattern with *Δx* (Fig. 5b). *DBA* values

268 range from 108,848 m^2 to 241,216 m^2, with an average of 163,635 m^2 over the whole

269 study period. Dry beach area values smaller than the average also mainly occurred in

270 autumn and winter when storm events were intensive.

271   The variation pattern of beach orientation is shown temporally in Fig. 5c.

272 Generally, abrupt variations in the beach orientation (caused by storm events or

273 nourishments) were always followed by gradual recoveries to 19.5° (the average beach

274 orientation). Beach rotation varied between a minimum value of -2.63° and a maximum

275 of 0.67°. Clear rotation was identified as counter-clockwise after March, 2017 when

276 storm events were sparse.

277   The unit width volumetric change highly depends on the alongshore position with

278 an average of -60.4 m^3/m and various patterns are present at the northern (transect 1-

279 10), middle (transect 11-20) and southern (transect 21-30) beach (Fig. 5d). It is shown

280 that the largest positive volumetric change occurred on transect 29 (488 m^3/m) and the

281 largest negative on transect 9 (-460 m^3/m). The overall variation of unit width volume

282 indicates a transition from erosion in the north to accretion in the south under calm

283 conditions, while the erosion of northern beach is more severe than the southern beach

284 after storm events. Averaged unit width volumetric changes are 14.4 m^3/m, -59.71 m^3/m,

285 -0.23 m^3/m, and 139.97 m^3/m in summer, autumn, winter and spring, respectively,

286 suggesting an seasonal variation pattern: slight accretion-severe erosion-slight erosion-

287   strong accretion. Most of the obvious accretion (erosion) peak values commonly

288   correspond to nourishments (storm events). In addition, the borrowed sediments were

289   mainly placed between transect 16-28 (Fig. 2), while the distribution of obvious

290   accretion peaks commonly ranged from transect 15-30, indicating the nourishment

291   impact on beach.
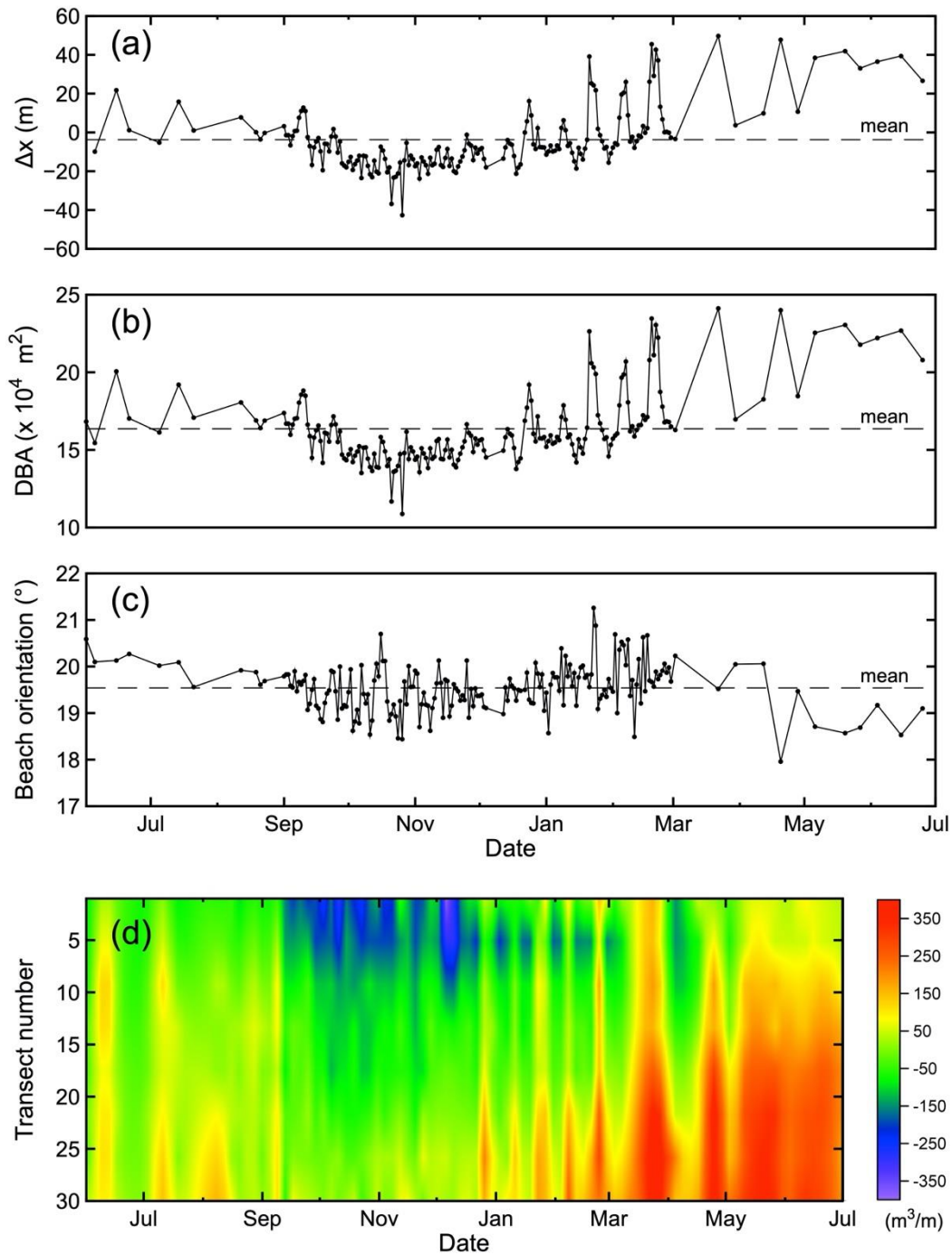
Fig. 5. Distribution of shoreline displacement (Δx) (**a**), dry beach area (*DBA*) (**b**), beach orientation (**c**) and unit width volumetric change (ΔV) (**d**) of Dongsha beach over the study period.

3.3. Beach responses to individual storm events

297 There were 19 storm events over the study period with various impacts on

298 Dongsha beach. Table 2 shows the Δx, change in dry beach area (ΔDBA), unit width

299 volumetric change (ΔV), and beach rotation during each storm event. Since most of the

300 storm events occurred along with beach nourishments, beach responses to individual

301 storm events are different and complex. According to the relationship between the

302 occurrence time of the storm events and nourishments, we divided beach responses (to

303 individual storm events) into five cases (Table 2). In Table 2, we chose the nourishment

304 event with the nearest occurrence time in depicting the occurrence time of each storm

305 event. E.g., if S3 occurred in 1 day after N1 and 4 days before N2, then the occurrence

306 time of S3 in Table 2 would be recognized as 1 day after N1.

307 ***Case1: Without nourishment***

308 Case1 includes the storm events occurred before the beginning of nourishment

309 projects (S1 and S2). The two storm events with moderate H_s in Case1 produced none

310 erosion but advances in shoreline (Table 2). In the meanwhile, beach rotation is not

311 significant in this case.

312 ***Case2: Nourishment occurred before storm event***

313 Case2 consists of the storm events occurred after nourishments (S3, S4, S6, S7,

314 S8, S9 S12, S14 and S15). S3 has the longest duration with the highest P_s of 1157.76

315 m^2h, but did not cause the most severe erosion. While S4 with the second higher P_s,

316 induced the severest beach erosion of 79.16 m^3/m and 15.83 m retreat in shoreline (Fig.

317 3 and Table 2). Different beach responses to S3, S4, S9 and S14 may correlate with

318   sand volume scale of nourishment projects. S3 and S9 occurred after two large sand

319   nourishments (~10000 m^3 and ~5000 m^3, respectively), while S4 and S14 occurred after

320   two small sand nourishments (~1000 m^3). Although nourishments implemented before

321   storm events can compensate for the sediment loss, the beach still lost a lot of sediments

322   after those four storm events. However, storm events identified as calm (S6, S7, S8,

323   S12, S15) occurred after nourishments did not cause erosion. The results of this case

324   show that nourishments before storm events can be effective only when the storm

325   energy is low. Beach rotation varied significantly in this case without regular pattern.

326   In the meanwhile, consecutive storm events did not show cumulative erosion in this

327   case.

328   *Case3: Nourishment occurred at the same time with storm event*

329   There were two pairs of storm events and nourishments happened at the same time:

330   N5 and S11, N6 and S13. The two storm events in this case showed no erosion but

331   accretion with the same volume (~5000 m^3) nourishments (Table 2). The different Δx

332   corresponds well to the different storm energy in this case: the higher the storm energy

333   is, the larger the shoreline displacement is.

334   *Case4: Nourishment occurred after storm event*

335   Three storm events (S5, S10, S17) in this case did not cause any erosion (Table 2).

336   Especially, S5 with a H_{max} of 3 m did not cause shoreline retreat, which might due to

337   the compensation of N5. The result shows that nourishments in this case compensated

338   the sediment loss effectively.

Case5: Long interval between storm event and nourishment

S18 and S19 occurred at the end of study period. S18 made no erosion but a 0.64° counter-clockwise beach rotation, while S19 caused a 12.75 m retreat in shoreline with a 0.57° clockwise beach rotation. Although the two storm events in this case had the similar E and P_s (Fig. 3), the impacts vary. Furthermore, the calm storm S19 caused significant erosion of the beach, and its erosion degree even exceeded S3, S9 and S14, indicating that the borrowing sediments before the storm event has compensated for the beach loss during those storm events. When there is no borrowed sediment to make up for the loss, a calm storm event like S19 can cause a shoreline retreat of more than 10 m.

Comparing the above five cases, we could get the results that the storm erosion can be fully compensated by sand nourishment no matter when the nourishment project occurred for storm events identified as calm ($P_s \leq 250$ m²h). Regarding moderate ($251 < P_s \leq 500$ m²h) and significant ($P_s > 500$ m²h) severity storm events, borrowing sediments timely after the storm event is the most effective way to maintain Dongsha beach. Although the beach did not show significant erosion when the storm events and nourishments occurred simultaneously, the nourishment effect was not so significant as in Case 4. Nourishments in Case1, Case2, Case3 and Case4 all have compensated for the storm erosion. However, the sediment loss caused by storm erosion cannot be compensated in Case5 due to the long interval between storm events and nourishments, which made the calm storm (e.g. S19) cause severe erosion.

360 **Table 2**

361 Morphological variations of Dongsha beach after individual storm events during the study period.

Case	Storm	H_{max} (m)	Occurrence Time (refer to Fig. 3)	ΔV (m³/m)	Δx (m)	ΔDBA (m²)	Rotation (°)	Recovery period (day)
1	S1	2.10	without nourishment	105.16	21.03	30704	0.07	/
1	S2	2.10	without nourishment	33.80	6.76	9862	0.37	/
2	S3	2.40	1 day after N1	-36.85	-7.37	-10839	0.42	no recovery
2	S4	3.10	2 days after N2	-79.16	-15.83	-23113	-0.33	no recovery
2	S6	1.60	1 day after N4	9.66	1.93	3812	-1.49	/
2	S7	1.60	4 days after N4	34.79	6.96	8455	1.16	/
2	S8	2.60	6 days after N4	26.28	5.26	7704	0.42	/
2	S9	2.80	14 days after N4	-37.82	-7.56	-9455	-1.66	no recovery
2	S12	1.70	7 days after N5	41.53	8.31	11988	-0.19	/
2	S14	1.50	2 days after N9	-41.78	-8.36	-12327	0.06	32
2	S15	2.80	21 days after N9	265.49	53.10	78313	-0.71	/
3	S11	2.10	at the same time with N5	3.65	0.73	909	0.14	/
3	S13	1.80	at the same time with N6	58.82	11.76	16375	0.63	/
4	S5	3.00	1 day before N4	2.98	0.60	1928	-1.17	/
4	S10	1.80	7 days before N5	36.71	7.34	10651	0.33	>13
4	S17	1.7	14 days before N10	138.85	27.77	40807	-0.76	/
5	S16	1.6	60 days after N9	-185.52	-37.1	-55230	1.51	24
5	S18	1.60	27 days after N10	14.54	2.91	4811	-0.64	/
5	S19	1.70	31 days after N10	-63.75	-12.75	-19046	0.57	>7

362

4. Discussion

4.1. Evaluation of beach nourishments

The effectiveness of sand nourishments in this study has been evaluated in terms of their abilities to meet the project goals, which were to prevent storm erosion and widen the recreational beach. As for preventing storm erosion, 12 storm events with none erosion and 3 storm events recovered within several days were observed (Table 2). However, seawall constructed on the beach and the intensive storm events resulted in long-term erosion. Guo et al. (2018) found that Dongsha beach didn't recover from a storm event during 2014 and 2015 without sand nourishment, suggesting that the nourishment projects in this study are successful in preventing storm erosion. In terms of widening the recreational beach, all the nourishment projects recorded increases in $\overline{DBW}$ and DBA. The maximum increases in $\overline{DBW}$ and DBA observed over the 10 nourishment periods are 50.18 m and 74755 m^2, respectively (Table 3). The relatively short duration of this study limited the assessment of longer-term benefits of the nourishments, the results only suggest that nourishments on Dongsha beach were successful in achieving these two goals over a year video monitoring.

Although nourishment on this beach have met the project goal, beach nourishments can often cause large-scale nearshore disturbances that affect the balance of alongshore and cross-shore sediment transport (Dean, 1983). In general, the sediment transport on the beach without human intervention is mainly controlled by the hydrodynamic processes(Wiggins et al., 2019) and beach characteristics (Oliveira et al., 2017). Sediment transport on the beach can be more complex with human activities

23

385   (Duvat et al., 2019; Luo et al., 2016). Cheng et al.(2014) found that significant erosion

386   in summer and accretion in winter were the main seasonal variation pattern of Dongsha

387   beach without nourishment, while the beach accreted in summer months with

388   nourishment in this study. In addition, the distribution of erosion/ accretion on Dongsha

389   beach also varies with and without nourishments. The beach used to be eroded in the

390   southern beach (Cheng et al., 2014), while significant accretion can be seen on the

391   southern beach with nourishment. The change of seasonal variation pattern and

392   erosion/accretion distribution on this beach may be related to the nourishment impacts,

393   and further study on sediment transport needs the support of sediment information.

394   Besides, longevities of the borrowed sediments in this study can only be

395   considered short compared with beach nourishments in Europe countries (Hamm et al.,

396   2002; Hanson et al., 2002) and the USA (Leonard et al., 1989). Generally, the larger

397   scale of volume produced the better effectiveness on both morphological variation and

398   longevity of borrowed sediments (Table 3). In the meanwhile, beach nourishment with

399   the largest volume did not always cause the largest increase in $\overline{DBW}/DBA$ and the

400   longest longevity due to the intensive storm events. For example, N1 with about 10000

401   m^3 borrowed sediments but only has a 3-day longevity. Although the borrowed

402   sediments limited in the tourist-dense area (Fig. 6) could meet the recreational need,

403   counter-clockwise rotation was identified after 9 nourishment projects. The advances

404   in southern shoreline resulting from the limited sand placement of borrowed sediments

405   might have contributed to the counter-clockwise rotation in this study. Long-term

24

406 erosion rates and its spatial gradient is a design guide for the beach nourishment project

407 (Kaczkowski et al., 2018), which the spatial location of borrowed sediments should

408 depend on. Limited alongshore position of sand placement and the implement timing

409 when storm events were intensive are the main causes of those inefficiencies in the

410 nourishments in this study.

411 Table 3

412 Beach nourishment longevity and morphological variations of Dongsha beach.

Nourishment	Sand volume (m^3)	Longevity (days)	$\Delta\overline{DBW}_{max}$ (m)	ΔDBA_{max} (m^2)	Beach rotation(°)
N1	~10000	3	5.20	7631	-0.18
N2	~1000	1	3.83	5551	-1.06
N3	~2000	2	3.32	3484	-0.47
N4	~5000	7	7.31	10198	0.09
N5	~10000	59	32.96	47496	-1.39
N6	~10000	8	16.07	24680	-0.27
N7	~2000	11	50.18	74755	-0.26
N8	~10000	18	41.56	61124	-0.98
N9	~1000	7	43.25	63539	-0.61
N10	~1000	3	3.45	5010	-0.15

413 Note: $\Delta\overline{DBW}_{max}$ is the max change in $\overline{DBW}$; ΔDBA_{max} is the max change in DBA.
414

415

Fig.6. A snap image taken by the Argus video monitoring system of sand being placed

on the beach (Image date: 12/09/2016 08:00 GMT).

4.2. Factors affecting nourishment longevity

The majority of nourishment projects have a longevity of several years in USA

(Leonard et al., 1989) and Europe countries (Hamm et al., 2002; Hanson et al., 2002).

However, in this study, the longevity of borrowed sediments can only last for several

days to tens of days (Table 3), which correlates well with the wave regime of the study

area. Frequent storms with high significant wave heights make the sediments difficult

to preserve (Table 2).

Besides, characteristic of the borrowed sediment can influence the longevity. The

larger volume scale of the borrowed sediments can often causes the longer nourishment

longevity (Cooke et al., 2012; Hamm et al., 2002; Hanson et al., 2002; Leonard et al.,

1989), and the different beach responses to individual storm events in Case2 showed

the similar result. Previous studies also showed that grain size distribution (Chiva et al.,

2018; Pranzini et al., 2018; Stauble, 2007), mineral component (Pagán et al., 2018) and

26

spatial location (Karambas and Samaras, 2014) can affect the nourishment longevity, which could not be obtained in this study due to the data limitation.

It is worth noting that different occurrence time of nourishments is also a significant factor affecting the longevity. Generally, nourishments occurred timely after storm events have longer longevity in this study (Table 3). Storm events with high significant wave heights can take away a great number of sediments on the beach (Coco et al., 2014; Harley et al., 2014; Qi et al., 2010; Scott et al., 2016; Senechal et al., 2015), and borrowed sediments might lose more easily than the native sediments during storm events (Seymour et al., 2005). Nourishments implemented timely after storm events can not only avoid strong hydrodynamic conditions, but also quickly compensate for losses caused by storm erosion. Thus, occurrence time can have significant impacts on the longevity of nourishment implemented on this beach.

4.3. *Implications of nourishment management*

Serious beach erosion is observed globally due to the climate change with sea level rise and more frequent and severe storms (Castelle et al., 2007; Houston and Dean, 2014; Qi et al., 2010; Scott et al., 2016; Smith et al., 2014). Under this circumstance, there are growing numbers of beach nourishments to meet increasing public requirements (Kuang et al., 2011). This kind of nourishment coupled with the consideration of nourishment occurrence time can be an effective way to restore the beach exposed to frequent storms. Also, placing borrowed sediments should consider the erosion distribution pattern to achieve better efficiency. Since the nourishment

452   projects were implemented with the same operations and cross-shore position in this

453   study, we can only suggest that placing the borrowed sediments on the erosion area

454   alongshore but not the limited easy-access area might cause better efficiency. Many

455   studies have predicted the evolution of different kinds of sand nourishments by

456   numerical simulation (Kuang et al., 2011; Pan, 2011), which may make the sand

457   nourishment more effective. Although the applicability of this work may be limited,

458   our results can provide a reference for beach management since this kind of

459   nourishment is common in the local area. Besides, this research can also provide a case

460   study for protecting eroded beaches around the world, but the implementation on other

461   beaches needs to consider their respective characteristics and local storm condition.

462   **5.   Conclusions**

463   Due to the increasing storm erosion of beaches, beach nourishment has become

464   a wide-used measure. Argus video monitoring system is an effective means to monitor

465   continuous storm-induced erosion of beaches and corresponding nourishment

466   effectiveness. In this case study of Dongsha beach, video-derived morphological

467   parameters of the beach were analyzed over a year, and the following main conclusions

468   are obtained.

469   Seasonal morphological variation related to storm-intensive period existed on this

470   beach. Shorelines retreated during autumn and winter when storms were intensive,

471   while advanced in spring and summer, with a lot of bulges occurred after nourishment

472   projects. Abrupt variations in the beach orientation were always followed by gradual

473 recoveries to the average, while continuous counter-clockwise rotation occurred after

474 March, 2017 when storm events were sparse.

475 The implementation of nourishment to prevent storm erosion on embayed beaches

476 should consider the occurrence time, borrowing sediments timely after the storm event

477 is the most effective way to compensate for storm erosion in this study. Unsuitable

478 timing and alongshore position of these nourishments might cause short longevity and

479 beach rotation. This study can provide a reference for sand nourishments on eroded

480 beaches, enabling beach management decisions to be implemented reasonably.

481

Declaration of interest

489 The authors report no conflicts of interest.

References

491 Aarninkhof, S.G.J., Turner, I.L., Dronkers, T.D.T., Caljouw, M., Nipius, L., 200
492   3. A video-based technique for mapping intertidal beach bathymetry. Coast.
493   Eng. 49, 275–289. https://doi.org/10.1016/S0378-3839(03)00064-4
494 Angnuureng, D.B., Almar, R., Senechal, N., Castelle, B., Addo, K.A., Marieu,
495   V., Ranasinghe, R., 2017. Shoreline resilience to individual storms and stor

m clusters on a meso-macrotidal barred beach. Geomorphology 290. https://doi.org/10.1016/j.geomorph.2017.04.007

Archetti, R., Paci, A., Carniel, S., Bonaldo, D., 2016. Optimal index related to the shoreline dynamics during a storm: the case of Jesolo beach. Nat. Hazards Earth Syst. Sci. 16, 1107–1122. https://doi.org/10.5194/nhess-16-1107-2016

Archetti, R., Romagnoli, C., 2011. Analysis of the effects of different storm events on shoreline dynamics of an artificially embayed beach. Earth Surf. Process. Landforms 36, 1449–1463. https://doi.org/10.1002/esp.2162

Balouin, Y., Tesson, J., Gervais, M., 2013. Cuspate shoreline relationship with nearshore bar dynamics during storm events – field observations at Sete beach, France. J. Coast. Res. 65, 440–445. https://doi.org/10.2112/SI65-075.1

Basterretxea, G., Orfila, A., Jordi, A., Fornós, J.J., Tintoré, J., 2007. Evaluation of a small volume renourishment strategy on a narrow Mediterranean beach. Geomorphology. https://doi.org/10.1016/j.geomorph.2006.10.019

Bird, E.C.F., 1985. Coastline Changes. A Global Review. John Wiley and Sons, Chichester.

Boccotti, P. (Ed.), 2000. Chapter 6 The Wave Climate, in: Wave Mechanics for Ocean Engineering. Elsevier, pp. 183–206. https://doi.org/10.1016/S0422-9894(00)80032-X

Cai, F., Dean, R.G., Liu, J., 2011. Beach nourishment in China: Status and prospects, in: Coastal Engineering Proceedings. p. 31. https://doi.org/10.9753/icce.v32.management.31

Castelle, B., Turner, I.L., Bertin, X., Tomlinson, R., 2009. Beach nourishments at Coolangatta Bay over the period 1987–2005: Impacts and lessons. Coast. Eng. 56, 940–950. https://doi.org/10.1016/j.coastaleng.2009.05.005

Castelle, B.O., Turner, I.L., Ruessink, B.G., Tomlinson, R.B., 2007. Impact of storms on beach erosion: broad beach (Gold Coast, Australia). J. Coast. Res. 23, 534–539.

Cheng, L., Shi, L., Xia, X., Tong, X., 2014. Sedimentation and recent morphological changes at Dongsha beach, Zhujiajian Island , Zhejiang Province. Mar. Geol. Quat. Geol. 34, 37–44.

Chiva, L., Pagán, J.I., López, I., Tenza-Abril, A.J., Aragonés, L., Sánchez, I., 2018. The effects of sediment used in beach nourishment: Study case El Portet de Moraira beach. Sci. Total Environ. 628–629, 64–73. https://doi.org/10.1016/j.scitotenv.2018.02.042

Coco, G., Senechal, N., Rejas, A., Bryan, K.R., Capo, S., Parisot, J.P., Brown,

533   J.A., MacMahan, J.H.M., 2014. Beach response to a sequence of extreme
534   storms. Geomorphology 204, 493–501. https://doi.org/10.1016/j.geomorph.20
535   13.08.028

536   Cooke, B.C., Jones, A.R., Goodwin, I.D., Bishop, M.J., 2012. Nourishment pra
537   ctices on Australian sandy beaches: A review. J. Environ. Manage. 113, 31
538   9–327. https://doi.org/10.1016/j.jenvman.2012.09.025

539   Dean, R.G., 1983. Principles of beach nourishment, in: CRC Handbook of Coa
540   stal Processes and Erosion. CRC Press, pp. 217–232.

541   Dolan, R., Davis, R.E., 1992. An intensity scale for Atlantic coast northeast st
542   orms. J. Coast. Res. 8, 840–853.

543   Duvat, V., Pillet, V., Volto, N., Krien, Y., Cécé, R., Bernard, D., 2019. High h
544   uman influence on beach response to tropical cyclones in small islands: Sa
545   int-Martin Island, Lesser Antilles. Geomorphology 325, 70–91. https://doi.or
546   g/10.1016/j.geomorph.2018.09.029

547   Elko, N.A., Holman, R.A., Gelfenbaum, G., 2005. Quantifying the Rapid Evolu
548   tion of a Nourishment Project with Video Imagery. J. Coast. Res. 214, 63
549   3–645. https://doi.org/10.2112/04-0280.1

550   Elko, N.A., Wang, P., 2007. Immediate profile and planform evolution of a bea
551   ch nourishment project with hurricane influences. Coast. Eng. 54, 49–66. h
552   ttps://doi.org/10.1016/j.coastaleng.2006.08.001

553   Guo, J., Shi, L., Chen, S., Ye, Q., 2019. Response of Dongsha beach in Zhous
554   han to continuous storms based on Argus images. Oceanol. Limnol. Sin. 5
555   0, 728–739. https://doi.org/10.11693/hyhz20181200285

556   Guo, J., Shi, L., Tong, X., Zheng, Y., Xu, D., 2018. The response to tropical
557   storm Nakri and the restoration of Dongsha Beach in Zhujiajian Island, Zh
558   ejiang Province. Haiyang Xuebao 40, 137–147. https://doi.org/10.3969 /j.iss
559   n.0253-4193.2018.09.012

560   Hamm, L., Capobianco, M., Dette, H.., Lechuga, A., Spanhoff, R., Stive, M.J..,
561   2002. A summary of European experience with shore nourishment. Coast.
562   Eng. 47, 237–264. https://doi.org/10.1016/S0378-3839(02)00127-8

563   Hanson, H., Brampton, A., Capobianco, M., Dette, H.., Hamm, L., Laustrup, C.,
564   Lechuga, A., Spanhoff, R., 2002. Beach nourishment projects, practices, a
565   nd objectives—a European overview. Coast. Eng. 47, 81–111. https://doi.or
566   g/10.1016/S0378-3839(02)00122-9

567   Harley, M.D., Andriolo, U., Armaroli, C., Ciavola, P., 2014. Shoreline rotation
568   and response to nourishment of a gravel embayed beach using a low-cost
569   video monitoring technique: San Michele-Sassi Neri, Central Italy. J. Coast.

Conserv. 18, 551–565. https://doi.org/10.1007/s11852-013-0292-x

Harley, M.D., Turner, I.L., Short, A.D., 2015. New insights into embayed beach rotation: The importance of wave exposure and cross-shore processes. J. Geophys. Res. Earth Surf. 120, 1470–1484. https://doi.org/10.1002/2014JF003390

Houston, J.R., Dean, R.G., 2014. Shoreline Change on the East Coast of Florida. J. Coast. Res. 30, 647. https://doi.org/10.2112/JCOASTRES-D-14-00028.1

Hu, R., Wu, J., Li, G., Zhu, L., Ma, F., 2009. Characteristics of sediment transport in the Zhoushan Archipelago sea area. Acta Oceanol. Sin. 28, 116–127.

Kaczkowski, H.L., Kana, T.W., Traynum, S.B., Visser, R., 2018. Beach-fill equilibration and dune growth at two large-scale nourishment sites. Ocean Dyn. 68, 1191–1206. https://doi.org/10.1007/s10236-018-1176-2

Karambas, T. V., Samaras, A.G., 2014. Soft shore protection methods: The use of advanced numerical models in the evaluation of beach nourishment. Ocean Eng. 92, 129–136. https://doi.org/10.1016/j.oceaneng.2014.09.043

Karunarathna, H., Brown, J., Chatzirodou, A., Dissanayake, P., Wisse, P., 2018. Multi-timescale morphological modelling of a dune-fronted sandy beach. Coast. Eng. 136, 161–171. https://doi.org/10.1016/j.coastaleng.2018.03.005

Karunarathna, H., Pender, D., Ranasinghe, R., Short, A.D., Reeve, D.E., 2014. The effects of storm clustering on beach profile variability. Mar. Geol. 348, 103–112. https://doi.org/10.1016/j.margeo.2013.12.007

Kuang, C., Mao, X., Gu, J., Niu, H., Ma, Y., Yang, Y., Qiu, R., Zhang, J., 2019. Morphological processes of two artificial submerged shore-parallel sand bars for beach nourishment in a nearshore zone. Ocean Coast. Manag. 179, 104870. https://doi.org/10.1016/j.ocecoaman.2019.104870

Kuang, C., Pan, Y., Zhangn, Y., Liu, S., Yang, Y., Zhang, J., Dong, P., 2011. Performance Evaluation of a Beach Nourishment Project at West Beach in Beidaihe, China. J. Coast. Res. 27, 769. https://doi.org/10.2112/JCOASTRES-D-10-00184.1

Leonard, L., Clayton, T.D., Dixon, K., Pilkey, O.H., 1989. U.S. beach replenishment experience. A comparison of the Atlantic, Pacific, and Gulf Coasts, in: Coastal Zone: Proceedings of the Symposium on Coastal and Ocean Management. pp. 1994–2006.

Li, G., Gao, S., Wang, Y., Li, C., 2018. Sediment flux from the Zhoushan Archipelago, eastern China. J. Geogr. Sci. https://doi.org/10.1007/s11442-018-1479-8

607   Liu, G., Cai, F., Qi, H., Zhu, J., Lei, G., Cao, H., Zheng, J., 2019. A method
608   to nourished beach stability assessment: The case of China. Ocean Coast.
609   Manag. 177, 166–178. https://doi.org/10.1016/j.ocecoaman.2019.05.015
610   Lu, J., 2010. Research Report on the Regional Climate of 908 Special Island
611   Survey in Zhejiang Province.
612   Luo, S., Liu, Y., Jin, R., Zhang, J., Wei, W., 2016. A guide to coastal manage
613   ment: Benefits and lessons learned of beach nourishment practices in Chin
614   a over the past two decades. Ocean Coast. Manag. 134, 207–215. https://d
615   oi.org/10.1016/j.ocecoaman.2016.10.011
616   Mendoza, E.T., Jimenez, J.A., Mateo, J., 2011. A coastal storms intensity scale
617   for the Catalan sea (NW Mediterranean). Nat. Hazards Earth Syst. Sci. 11,
618   2453–2462. https://doi.org/10.5194/nhess-11-2453-2011
619   Ojeda, E., Guillén, J., 2008. Shoreline dynamics and beach rotation of artificial
620   embayed beaches. Mar. Geol. 253, 51–62. https://doi.org/10.1016/j.margeo.
621   2008.03.010
622   Oliveira, S., Moura, D., Horta, J., Nascimento, A., Gomes, A., Veiga-Pires, C.,
623   2017. The morphosedimentary behaviour of a headland–beach system: Qua
624   ntifying sediment transport using fluorescent tracers. Mar. Geol. 388, 62–7
625   3. https://doi.org/10.1016/j.margeo.2017.02.010
626   Pagán, J.I., López, M., López, I., Tenza-Abril, A.J., Aragonés, L., 2018. Study
627   of the evolution of gravel beaches nourished with sand. Sci. Total Environ.
628   626, 87–95. https://doi.org/10.1016/j.scitotenv.2018.01.015
629   Pan, S., 2011. Modelling beach nourishment under macro-tide conditions. J. Co
630   ast. Res. 64, 2063–2067.
631   Pranzini, E., Anfuso, G., Muñoz-Perez, J.J., 2018. A probabilistic approach to
632   borrow sediment selection in beach nourishment projects. Coast. Eng. 139,
633   32–35. https://doi.org/10.1016/j.coastaleng.2018.05.001
634   Psuty, N.P., Moreira, M.E.S.A., 1992. Characteristics and longevity of beach no
635   urishment at Praia da Rocha, Portugal. J. Coast. Res. 8, 660–676.
636   Qi, H., Cai, F., Lei, G., Cao, H., Shi, F., 2010. The response of three main b
637   each types to tropical storms in South China. Mar. Geol. https://doi.org/10.
638   1016/j.margeo.2010.06.005
639   Scott, T., Masselink, G., O'Hare, T., Saulter, A., Poate, T., Russell, P., Davidso
640   n, M., Conley, D., 2016. The extreme 2013/2014 winter storms: Beach rec
641   overy along the southwest coast of England. Mar. Geol. 382, 224–241. htt
642   ps://doi.org/10.1016/j.margeo.2016.10.011
643   Senechal, N., Coco, G., Castelle, B., Marieu, V., 2015. Storm impact on the se

asonal shoreline dynamics of a meso- to macrotidal open sandy beach (Biscarrosse, France). Geomorphology 228, 448–461. https://doi.org/10.1016/j.geomorph.2014.09.025

Seymour, R., Guza, R.T., O'Reilly, W., Elgar, S., 2005. Rapid erosion of a small southern California beach fill. Coast. Eng. 52, 151–158. https://doi.org/10.1016/j.coastaleng.2004.10.003

Short, Andrew D., Masselink, G., 1999. Embayed and structurally controlled beaches, in: Short, A.D. (Ed.), Handbook of Beach and Shoreface Morphodynamics. John Wiley and Sons Ltd., Chichester, pp. 230–250.

Smith, A.M.M., Guastella, L.A.A., Botes, Z.A.A., Bundy, S.C.C., Mather, A.A.A., 2014. Forecasting cyclic coastal erosion on a multi-annual to multi-decadal scale: Southeast African coast. Estuar. Coast. Shelf Sci. 150, 86–91. https://doi.org/10.1016/j.ecss.2013.12.010

Stauble, D.K., 2007. Assessing beach fill compatibility through project performance evaluation, in: Coastal Sediments '07. American Society of Civil Engineers, Reston, VA, pp. 2418–2431. https://doi.org/10.1061/40926(239)190

Stauble, D.K., 1988. Beach nourishment monitoring, a necessity to project design. Beach Preserv. Technol. 88 Probl. Adv. Beach Nourishment 88, 87–98.

Third Institute of Oceanography, 2010. Coast erosion assessment and control: The final investigation and assessment.

Wiggins, M., Scott, T., Masselink, G., Russell, P., McCarroll, R.J., 2019. Coastal embayment rotation: Response to extreme events and climate control, using full embayment surveys. Geomorphology. https://doi.org/10.1016/j.geomorph.2018.11.014

Xia, X., 2014. China's Islands: Zhejiang (Volume II: Zhoushan Archipelago). China Ocean Press, Beijing.